

# Thermodynamic properties of Holstein polarons and the effects of disorder

A. N. Das <sup>a</sup> and S. Sil <sup>b</sup>

<sup>a</sup> *Theoretical Condensed Matter Physics Division, Saha Institute of Nuclear Physics,  
1/AF, Bidhannagar, Kolkata 700064, India*

<sup>b</sup> *Department of Physics, Visva Bharati, Santiniketan- 731 235, India*

The ground state and finite temperature properties of polarons are studied considering a two-site and a four-site Holstein model by exact diagonalization of the Hamiltonian. The kinetic energy, Drude weight, correlation functions involving charge and lattice deformations, and the specific heat have been evaluated as a function of electron-phonon ( $e$ - $ph$ ) coupling strength and temperature. The effects of site diagonal disorder on the above properties have been investigated. The disorder is found to suppress the kinetic energy and the Drude weight, reduces the spatial extension of the polaron, and makes the large-to-small polaron crossover smoother. Increasing temperature also plays similar role. For strong coupling the kinetic energy arises mainly from the incoherent hopping processes owing to the motion of electrons within the polaron and is almost independent of the disorder strength. From the coherent and incoherent contributions to the kinetic energy, the temperature above which the incoherent part dominates is determined as a function of  $e$ - $ph$  coupling strength.

## I. Introduction

Study of different properties of polarons has been of great importance since the evidence of polaronic charge carriers in many materials of recent interest, viz. high- $T_c$  cuprates<sup>1</sup>, CMR-manganites<sup>2</sup>, biological materials like DNA<sup>3</sup>, etc. which have large technological potential and importance. In the simplest Holstein model an electron in a narrow tight-binding band interacts locally with dispersionless optical phonons. For large  $e$ - $ph$  coupling the resultant polaron is a small polaron with high effective mass, while for weak coupling it becomes a large polaron having a much lower effective mass for a finite adiabatic parameter. The crossover from a large to a small polaron and the corresponding changes in the polaronic properties in the ground state have been studied for the Holstein model by different groups<sup>4-14</sup> using various methods to enrich our understanding in this field. However, finite temperature study of the properties of polarons and the effect of disorder on polaronic properties are few and needs more attention. Previously we have studied the effect of disorder on some of the polaronic ground state properties (*i*) for a two-site system following a perturbation method based on a modified Lang-Firsov (MLF) phonon basis<sup>15</sup> and (*ii*) for a many-site system following a zero-phonon averaging of the MLF-transformed hamiltonian and a real space renormalization group method to deal with the disorder<sup>16</sup>. The above studies have the limitations that they are only for the ground state. The first study, though quite accurate, has been carried out only for a two-site system, while the latter study gives approximate results. In this paper we will consider a two-site and a four-site Holstein model and follow an exact diagonalization method to study the ground state as well as finite temperature properties of the polarons and the effect of disorder on them. We will mainly study the kinetic energy, correlation functions involving charge and lattice deformations, Drude weight and the specific heat of the systems as a function of  $e$ - $ph$  coupling for different

temperatures and disorder strength.

The paper is organized as follows. In Section II we have developed the formalism for the aforementioned study considering the Holstein model. We have presented the results and discussions for the two-site Holstein model in Section III-A and those for the four-site system in Section III-B. The conclusion is given in Section IV. In Appendix-A we have shown analytically considering an infinite size system and following strong-coupling second order perturbation theory that the disorder has weak or negligible effect on the kinetic energy for strong coupling.

## II. Formalism

The Holstein Hamiltonian with site diagonal disorder in 1-d is given by

$$H = \sum_i \epsilon_i c_i^\dagger c_i - \sum_i (t c_i^\dagger c_{i+1} + h.c) + g\omega \sum_i n_i (b_i^\dagger + b_i) + \omega \sum_i b_i^\dagger b_i \quad (1)$$

$c_i^\dagger$  and  $c_i$  are the electron creation and annihilation operators at the site  $i$ ,  $n_i (= c_i^\dagger c_i)$  is the number operator,  $b_i^\dagger$  and  $b_i$  are the creation and annihilation operators for the phonons corresponding to interatomic vibrations at site  $i$  and  $\omega$  is the phonon frequency. Electronic hopping takes place only between the nearest-neighbor sites with hopping strength  $t$  and  $g$  denotes the local  $e$ - $ph$  coupling. The electronic site energy  $\epsilon_i$  is independent of the site  $i$  for the ordered case. To study the effect of the site-diagonal disorder we would put a different site potential at one of the sites of the 2- or 4-site system. Spin index is not used for the electron, because a single polaron case has been studied here.

The third and fourth terms of Eq.1 represent the electron-phonon interaction and phonon harmonic energy, respectively. These terms may be written in the

momentum space defined by the phonon creation operators:  $b_{\mathbf{q}}^\dagger = (1/\sqrt{N}) \sum_i b_i^\dagger e^{i\mathbf{q}\cdot\mathbf{R}_i}$  and the corresponding annihilation operators, where  $N$  is the number of sites in the system<sup>5,6,14</sup>. It can be easily shown that the in-phase ( $\mathbf{q} = 0$ ) phonon mode does not couple with the electron dynamics but with the total number of electrons of the system. The harmonic term of this phonon mode along with its interaction with the electron may be separated out and written in a diagonal form<sup>5,6</sup>. The rest of the Hamiltonian involving  $(N-1)$  phonon modes and  $N$  electronic states (for a single electron problem) are considered to construct the eigen basis and matrix elements for diagonalization of the matrix. If one considers  $n_p$  number of phonon states per mode then the total number of basis states will be  $n_{Tot} = Nn_p^{(N-1)}$ . Elimination of the in-phase mode, thus, reduces the states of the Hilbert space by a factor of  $n_p$ , which is an advantage for any diagonalization procedure.

For the electron states we use the site space basis, which is convenient to take into account of the site disorder. For the phonon states we use the momentum space basis so that the in-phase ( $\mathbf{q} = \mathbf{0}$ ) mode may be separated out. The Hamiltonian is then diagonalized to obtain the eigenstates and the eigenenergies. Thermodynamic expectation value of any observable characterized by the operator  $O$  is then found out by

$$\langle O \rangle = \frac{1}{Z} \sum_{n=1}^{n_{Tot}} \langle n|O|n \rangle e^{-\beta E_n} \quad (2)$$

$$Z = \sum_{n=1}^{n_{Tot}} e^{-\beta E_n} \quad (3)$$

where  $E_n$  is the eigen energy of the  $n$ -th eigenstate  $|n\rangle$ ,  $\beta = 1/k_B T$  and  $T$  denotes the temperature. In this paper we are interested in evaluating the kinetic energy, static correlation function involving charge and lattice deformation, specific heat and the Drude weight. The operator corresponding to the kinetic energy is

$$H_t = -t \sum_{i,j} c_i^\dagger c_j. \quad (4)$$

For the correlation functions involving charge and lattice deformations we calculate

$$\chi_m(i) = \langle n_i (b_{i+m}^\dagger + b_{i+m}) \rangle / 2g \quad (5)$$

which represents the lattice deformation produced at the site  $i+m$  when the electron is at site  $i$ . The Drude weight ( $D_n$ ) in units of  $\pi e^2$  for an eigenstate  $|n\rangle$  of the polaronic system is obtained by introducing a phase factor to the hopping matrix element ( $t \rightarrow t e^{i\phi}$ ) in order to break the time reversal symmetry and then finding out the response of the break down of the time reversal symmetry to the electric current as<sup>17</sup>

$$D_n = \left. \frac{\partial^2 E_n(\phi)}{\partial \phi^2} \right|_{\phi=0} \quad (6)$$

where  $E_n(\phi)$  is the eigen energy of the  $n$ -th eigenstate in presence of non zero  $\phi$ . The thermodynamic expectation value of the Drude weight ( $D$ ) is found out by taking the thermal average of  $D_n$  over all the eigen states

$$\langle D \rangle = \frac{1}{Z} \sum_n D_n e^{-\beta E_n} \quad (7)$$

The specific heat may be expressed in terms of the energy fluctuation of the system at a finite temperature  $T$  as

$$C_v/k_B = \frac{1}{(k_B T)^2} [\langle E^2 \rangle - \langle E \rangle^2] \quad (8)$$

where  $\langle E \rangle$  and  $\langle E^2 \rangle$  are the thermal average of the energy and the square of the energy respectively.

### III. Results and discussions

#### A. Two-site system :

For the 2-site system the electron dynamics is coupled only to the out-of-phase ( $\mathbf{q} = \pi$ ) phonon mode. The Hamiltonian, which has to be considered for numerical diagonalization, is<sup>15</sup>

$$H_d = \sum_i \epsilon_i n_i - t(c_1^\dagger c_2 + c_2^\dagger c_1) + \omega g_+(n_1 - n_2)(d + d^\dagger) + \omega d^\dagger d \quad (9)$$

where  $g_+ = g/\sqrt{2}$  and  $d = (b_1 - b_2)/\sqrt{2}$ . We consider the basis states  $c_i^\dagger |0\rangle_e |n_d\rangle_{ph}$ , where  $i=1,2$  and  $n_d = 0, 1, 2, \dots, n_d^m$ , is the number of phonons in the d-oscillator. We refer to this as the bare basis. The Lang-Firsov transformed or MLF-transformed basis for the d-oscillators may also be used for diagonalization. But the matrix elements of the Hamiltonian operator are much simpler in the bare basis than those in other (LF or MLF) basis. We find that for exact diagonalization study the convergence of the results is achieved with much less number of phonon states within the bare basis compared to the LF or MLF basis, although the MLF basis is best and much better than the bare basis for perturbation calculation<sup>12</sup>.

To show the convergence of the correlation functions in the bare basis we have evaluated  $\langle n_1 u_2 \rangle$ , where  $u_2 = (b_2 + b_2^\dagger)$ , using different values of  $n_p$ , and plotted it as a function of  $g_+$  for different values of  $t$  and  $\epsilon_d (= \epsilon_2 - \epsilon_1)$  in Fig.1. We will refer to  $\epsilon_d$  for the two-site system as the disorder strength since it partly mimics the role of disorder in larger systems. It is found that in the range  $0 \leq g_+ \leq 3.2$  the results obtained for  $n_p = 25$  is quite accurate. The results for  $n_p = 25, 30$  and  $40$  are indistinguishable. We also find that for a particular value of  $n_p$  the highest value of  $g_+$ , up to which the convergence

is achieved, almost does not depend on  $\epsilon_d$  or  $t$  (Fig.1) in the range of parameters we have studied.

In Fig. 2 we have plotted the kinetic energy evaluated for the parameters  $t=1$  and  $\epsilon_d=1$ , using different values of  $n_p$ . It is found that the curves are indistinguishable for  $n_p \geq 15$  in the range  $0 < g_+ < 3.2$ . It shows that a much smaller value of  $n_p$  is sufficient to achieve the convergence in the kinetic energy than that for the convergence in the correlation function  $\langle n_1(b_2 + b_2^\dagger) \rangle$ . In the following we will present the results for the two-site system for  $n_p=40$  or 50. The latter is used for high temperature and strong coupling.

In Fig. 3 we have presented the variation of the correlation function  $\chi_m(i) = \langle n_i u_{i+m} \rangle / 2g$  for  $i=1,2$  and  $m=0,1$  for the parameters  $t = 2.1$  and  $\epsilon_d = 1$ . In the absence of disorder  $\chi_m(i)$  is independent of  $i$ . An introduction of the disorder ( $\epsilon_d \neq 0$ ) breaks the translational symmetry of the system and  $\chi_0(1)$  and  $\chi_0(2)$  become different such that  $\chi_0(1) - \chi_0(2)$  increases with the increase of the strength of the disorder potential ( $\epsilon_d$ ). However, it is observed that  $\langle n_1 u_2 \rangle = \langle n_2 u_1 \rangle$  even in the presence of disorder. For a periodic Holstein model the on-site correlation involving charge and lattice deformation  $\langle n_i u_i \rangle$  is always larger than the intersite correlation  $\langle n_i u_{i\pm 1} \rangle$ . With increasing  $e-ph$  coupling  $\langle n_i u_i \rangle$  increases while  $\langle n_i u_{i\pm 1} \rangle$  decreases indicating a crossover from a large polaron to a small polaron. In Fig.3 it is seen that in presence of disorder the correlation  $\langle n_2 u_2 \rangle$  decreases with increasing  $e-ph$  coupling and in the strong coupling region  $\langle n_2 u_2 \rangle < \langle n_2 u_1 \rangle$ . These are very different from the normal behavior of polarons in ordered systems. However,  $\langle n_1 u_1 \rangle$  and  $\langle n_1 u_2 \rangle$  show the usual characteristics of the polaron crossover with increasing  $e-ph$  coupling. The above-mentioned observations create confusion in distinguishing the large and small polaron from the structure of the correlation function  $\chi_m(i)$  in the disordered polaronic system. In this situation we define average correlation functions

$$\chi_0^{avg} = \frac{\sum_i \chi_0(i)}{\sum_i n_i} \quad (10)$$

$$\chi_1^{avg} = \frac{\sum_i \chi_1(i)}{\sum_i n_i} \quad (11)$$

$$\chi_d^{avg} = \frac{\sum_i (\chi_0(i) - \chi_1(i))}{\sum_i n_i} \quad (12)$$

to describe the polaronic behavior for the disordered polaronic system.

In Fig. 4 we have shown the variations of the kinetic energy and  $\chi_d^{avg}$  with  $g_+$  for  $t = 2.1$  for different values of  $\epsilon_d$ . It is seen that the kinetic energy is suppressed with increasing  $e-ph$  coupling as well as with increasing disorder strength. In the intermediate range of coupling the kinetic energy shows an exponential suppression. For strong coupling the kinetic energy shows a  $1/g^2$  behavior and is almost independent of the disorder strength, as noted previously<sup>15</sup>. In the Appendix-A, considering

an infinite lattice Holstein model we have shown analytically that for strong coupling the polaronic hopping is so small that the kinetic energy arises mainly from incoherent hopping owing to the undirected motion of the electron keeping the centre of the polaron fixed. This incoherent hopping contribution for large  $g$  is almost independent of the disorder strength and inversely proportional to  $g^2$ . Fig. 4 shows that with increasing disorder strength the correlation  $\chi_d^{avg}$  increases, which indicates that the size of the polaron becomes smaller, and the crossover (from a large to a small polaron) occurs at a lower value of  $g_+$ . For strong coupling, disorder has almost no effect on  $\chi_d^{avg}$  as similar to that observed for the kinetic energy. It may be noted that increasing disorder strength makes the polaron crossover more smoother.

To examine the effect of temperature on the properties of polarons we have evaluated the kinetic energy and the correlation function for different temperatures and disorder strength. In Figs. 5 and 6 we have plotted  $\chi_d^{avg}$  and the kinetic energy for  $t = 2.1$  as a function of  $g_+$  for different temperatures. For weak and intermediate coupling  $\chi_d^{avg}$  increases, implying that the size of the polaron becomes smaller, while the kinetic energy is suppressed with increasing temperature. For stronger coupling ( $g_+ > 1.7$ ) the temperature has an opposite effect, *i.e.*, the kinetic energy increases with temperature. However, the effect of temperature is small for strong coupling. At high temperature the variation of the kinetic energy with  $e-ph$  coupling is much weaker compared to that at low temperatures. It is also found that disorder has very little effect on both the kinetic energy and the correlation function at high temperatures (not shown in the figure).

We have studied the specific heat ( $C_v$ ) of the ordered as well as disordered polaronic system for different temperatures and hopping. In Fig. 7. we have presented the  $C_v$  of the ordered two-site system as a function of  $e-ph$  coupling for different temperatures for the hopping parameter  $t=2.1$ . Similar plots for different disorder strengths ( $\epsilon_d = 0, 0.5$  and  $1.0$ ), and for  $t=1$  and  $2.1$  are shown in Fig.8.

Fig.7 shows that in the low temperature regime the specific heat shows a peak at intermediate coupling. With increasing temperature the peak shifts towards a lower value of  $g_+$  and then disappears while a dip is developed in the intermediate coupling region. At low temperatures the specific heat is mainly governed by the separation of the ground state and the first excited state of the two-site Holstein model.

It may be noted that the specific heat for a system having only two energy levels with energy separation ( $\Delta E$ ), shows a peak at  $\Delta E/k_B T = 2.58$ , and  $C_v$  is very small when  $\Delta E$  is far from  $2.58k_B T$ . For the two-site Holstein model the energy separation ( $\Delta E$ ) between two lowest eigen energy levels decreases monotonically with  $g_+$  and becomes negligibly small at strong coupling<sup>18</sup>. At very low temperatures  $C_v$  is very small for weak  $e-ph$  coupling, as  $\Delta E/k_B T$  is sufficiently large.  $C_v$  attains a maxima

at an intermediate coupling, when  $\Delta E$  is  $\sim 2.58k_B T$ , and becomes very small in the strong coupling region as  $\Delta E \rightarrow 0$ . At a higher temperature a higher value of  $\Delta E$  is required to achieve the maximum value in  $C_v$ . Since  $\Delta E$  increases with decreasing  $g_+$  for the two-site Holstein model, the peak in  $C_v$  is obtained at a lower value of  $g_+$  for a higher temperature. With increasing temperature the higher energy states, in addition to the ground and first excited states, have significant contributions to the specific heat. This leads to the absence of the peak and formation of a dip in  $C_v$ . In Fig. 8 a comparison of the variation of specific heat as a function of  $g_+$  for the hopping parameters  $t = 1$  and  $2.1$  is given. In absence of any disorder the energy separation  $\Delta E$  increases with the increase of the hopping parameter  $t$ , hence a shift in the position of the peak in  $C_v$  is obtained at a higher value of  $g_+$ .

The effect of disorder on the specific heat of a polaron is also shown in Fig. 8. In presence of disorder the specific heat is suppressed for weak and intermediate coupling. However, for strong coupling the  $C_v$  is larger compared to that for the ordered case.

## B. Four-site system :

For the four site Holstein model, out of the four phonon modes there are three modes with  $\mathbf{q} \neq 0$  which couple to the electron dynamics. The four-site Holstein model Hamiltonian may be divided into two parts: one part containing the electronic terms, harmonic terms of the three phonon modes and the interaction of these phonon modes with the electron number operators, while the second part gives a diagonal form for the shifted in-phase ( $\mathbf{q} = 0$ ) oscillator (see Eqs. 7 and 8 of Ref.6). The first part, which contains the non trivial physics of the system and cannot be treated exactly by any analytical method, is diagonalized numerically. We have done the numerical diagonalization with  $n_p=9$  per phonon mode and checked that this gives fairly accurate results in the range of our study presented here. For the disordered case we break the translational symmetry by introducing a different site-potential at one of the lattice sites while keeping the equal site-potential for the rest.

For the Holstein model the correlation functions satisfy a sum rule

$$\begin{aligned} \sum_m \chi_m(i) &= \sum_m \langle n_i u_{i+m} \rangle / 2g \\ &= \langle n_i \rangle \end{aligned} \quad (13)$$

In absence of disorder  $\langle n_i u_j \rangle = \langle n_j u_i \rangle$  because of translational symmetry and a relation  $\sum_i \langle n_i u_j \rangle / 2g = \langle n_j \rangle$  is satisfied. We find that even for the disordered Holstein model  $\langle n_i u_j \rangle = \langle n_j u_i \rangle$ , though the sites  $i$  and  $j$  have different site potentials, and the relation  $\sum_i \langle n_i u_j \rangle / 2g = \langle n_j \rangle$  is also satisfied for the disordered system in addition to the sum rule (13). As mentioned previously average

correlation functions should be used for the disordered case to characterize the nature (large or small) of the polaron. Averaging also justifies that the disordered impurity may occupy any site at random. The average correlation functions involving charge and lattice deformations are:

$$\chi_m^{avg} = \frac{\sum_i \chi_m(i)}{\sum_i n_i} \quad (14)$$

where  $m = 0, 1, 2$ .

In Fig. 9 we have plotted the kinetic energy (scaled to  $2t$ ) and  $\chi_0^{avg}$  against  $g$  for the ordered case and for disordered cases with site potentials  $(1,0,0,0)$  and  $(-1,0,0,0)$ , where the values of the site potentials ( $\epsilon_i$ ) for  $i = 1, 2, 3, 4$  are shown within the parentheses (all the energies are expressed in units of  $\omega = 1$ ). It is seen that the polaron becomes more localized (in size) with higher value of  $\chi_0^{avg}$  and lower kinetic energy for disordered cases compared to the ordered case. For the  $(-1,0,0,0)$  case the value of  $\chi_0^{avg}$  is much higher and the kinetic energy is much lower than those for the  $(1,0,0,0)$  case, because in the former case the electron will tend to be trapped at the site of the negative potential. This would suppress the kinetic energy and favor small polaron formation in presence of  $e-ph$  coupling. In the same figure we have also shown the variations of  $\chi_1$  and  $\chi_2$  for the ordered case.  $\chi_1$  and  $\chi_2$  represent the lattice deformations produced at the nearest- and next-nearest neighbor sites of an electron. For small  $g$  the values of  $\chi_1$  and  $\chi_2$  are appreciable indicating that the polaron has spread over the lattice. With increasing  $g$ ,  $\chi_1$  and  $\chi_2$  reduce and become very small for strong coupling, the corresponding polaron is a small one. For the disordered cases the  $\chi_1^{avg}$  and  $\chi_2^{avg}$  behave in the same way (not shown in the figure), but their values are lower than those for the ordered case and become insignificant at a lower value of  $g$  compared to the ordered case. In the strong coupling limit the dependence of the kinetic energy and the correlation function on the disorder strength is very weak. The reasons have been explained in Appendix-A.

We have studied the effect of temperature on the correlation functions  $\chi_0$ ,  $\chi_1$  and  $\chi_2$  and on the kinetic energy. Fig.10 shows the variation of the on-site correlation function ( $\chi_0$ ) and the kinetic energy ( $-\langle K \rangle$ ) with temperature for different  $g$  values. Except for strong coupling the  $\chi_0$  increases while the kinetic energy decreases with increasing temperature. It may be noted that when  $\chi_0$  increases, the values of  $\chi_1$  and  $\chi_2$  decrease and the polaron size becomes smaller. For strong coupling the effect of temperature is small but opposite. The above behavior point to the fact that the polaron gets more and more localized with increasing temperature in the regime of weak and intermediate  $e-ph$  coupling, while for very strong coupling the polaron size gets larger with increasing temperature. We have also studied the properties of the ground state and different excited states individually to get a clear understanding of the observed temperature

variation. It is found that in the regime of weak and intermediate coupling the value of  $\chi_0$  is larger while the kinetic energy is smaller for the excited states compared to those of the ground state and this leads to increase (decrease) of  $\chi_0$  ( $-\langle K \rangle$ ) with increasing temperature. We have given a representative plot showing the variation of  $\chi_0$  with energy for the ground and the excited states for  $g = 1$  in Fig. 11. For strong coupling ( $g \geq 2.5$ ) we find that the  $\chi_0$  is smaller for the excited states (in general) than that for the ground state and the polaron becomes a larger polaron with increasing temperature.

For a fixed temperature  $\chi_0$  increases and the kinetic energy decreases with increasing  $g$  (Fig. 10), but their variation with  $g$  is much slower at higher temperatures. These results are qualitatively similar to that noted for the two-site system. It may be mentioned that Hohenadler<sup>19</sup> studied the 1-d Holstein model by quantum Monte Carlo method and observed similar variation of the kinetic energy with increasing temperature.

In Fig. 12 we have shown the variation of  $C_v$  as a function of  $g$  for the ordered and disordered systems for  $T = 0.1$ . The specific heat shows a peak at intermediate coupling, which is suppressed with increasing disorder strength. The behavior of  $C_v$  for the site potentials  $(-0.5, 0, 0)$  is similar to that observed for the 2-site case with  $\epsilon_d = 0.5$ . In Fig. 12 we have also shown the plots of  $\chi_0^{avg}$  to show that the specific heat peak occurs in the region of  $g$  where  $\chi_0^{avg}$  also undergoes a sharp change. However, the peak position in  $C_v$ , as mentioned previously, would be mainly decided by the tuning of the energy separation of two lowest levels of the system with the thermal energy at low temperatures.

The kinetic energy contains contributions from both the coherent and incoherent hopping processes<sup>20</sup>. The Drude weight (in units of  $\pi e^2$ ) represents the coherent part of the kinetic energy. The contribution from the incoherent hopping processes may be found out from the total kinetic energy and the Drude weight by using the f-sum rule (see appendix B),

$$-\frac{\langle K \rangle}{2} = \frac{\langle D \rangle}{2} + \langle S^{reg} \rangle \quad (15)$$

where,  $\langle K \rangle$  and  $\langle D \rangle$  are the thermal average of the kinetic energy and the Drude weight, respectively, and

$$S^{reg} = t^2 \sum_{n' \neq n} \frac{|\langle n | \sum_i (c_i^\dagger c_{i+1} - c_{i+1}^\dagger c_i) | n' \rangle|^2}{E_n - E_{n'}} \quad (16)$$

is proportional to the contribution to the kinetic energy from the incoherent hopping processes.

In Fig. 13 we have shown the effect of disorder on the Drude weight of the four-site Holstein model for  $t = 0.5$ . The kinetic energy and the Drude weight are plotted against  $g$  for the ordered and disordered systems. At  $g=0$ , the Drude weight and the kinetic energy have same values for the ordered case indicating that in absence of  $e$ - $ph$  interaction and disorder the entire part of the kinetic

energy comes from coherent hopping. In the range of intermediate to strong coupling the Drude weight shows an exponential suppression. The kinetic energy, on the other hand, shows an exponential suppression only in the range of intermediate coupling and a  $1/g^2$  behavior in the strong coupling region, as predicted by the strong coupling perturbation theory. For the disordered case the Drude weight is smaller than the kinetic energy even at  $g=0$ , because of disorder-induced incoherent hopping.

We have investigated the effect of temperature on the coherent and incoherent parts of the kinetic energy by evaluating the kinetic energy and the Drude weight as a function of temperature for different values of  $g$ . Some representative plots (for  $g=0.1, 0.5, 1$  and  $1.5$ ) are given in Fig.14. At low temperature the kinetic energy as well as the Drude weight show negligible dependence on temperature, represented by the flat region of the curves. This flat region is larger for smaller  $g$ . After the flat region the kinetic energy reduces exponentially with temperature. At high temperatures, where the Drude weight is very small, the kinetic energy may be fitted to a function  $a/T + bT$ . For small value of  $g$  the value of  $b$  is very small and the kinetic energy varies approximately as  $1/T$ . In the temperature range  $1.5 \leq k_B T \leq 2.5$  the values of  $a$  and  $b$  are, respectively, 0.477 and 0.003 for  $g = 0.1$ , 0.450 and 0.0054 for  $g = 0.5$ , 0.376 and 0.012 for  $g = 1.0$  and 0.281 and 0.020 for  $g = 1.5$ . The Drude weight shows almost exponential dependence on temperature both in the intermediate and high temperature range. A good fit to the Drude weight is obtained with a function  $ae^{-bT}$ , but with different values of the parameters  $a$  and  $b$  in the two (intermediate and high temperature) ranges.

The incoherent part of the kinetic energy can be directly determined from the difference between the negative kinetic energy and the Drude weight. In Fig. 14 we have also shown the variation of the incoherent part as a function of temperature for different  $g$  values. Except for very strong coupling (not shown in the figure) the incoherent part increases with temperature, reaches a peak and then decreases at a slow rate with increasing temperature. A cross-over temperature ( $T_{cross}$ ) may be defined from the intersection of the curves for the coherent and the incoherent part of the kinetic energy such that for  $T < T_{cross}$  the coherent part is dominant and for  $T > T_{cross}$  the incoherent part is dominant. We have plotted the variation of  $T_{cross}$  with  $g$  in Fig. 15. The cross-over temperature decreases with  $g$ . The  $T_{cross}$  vs.  $g$  curve shows a sudden change in the gradient at  $g=1$  for  $t = 0.5$ . The rate of fall of  $T_{cross}$  with  $g$  is higher in the region  $g > 1$  than that for  $g < 1$ .

To get the combined effect of the temperature and the disorder we have studied the Drude weight and incoherent part of the kinetic energy as a function of temperature for the site potentials  $(0,0,0,0)$  and  $(-1,0,0,0)$ . In Fig.16 we have given such a plot for intermediate coupling ( $g = 1$ ) where the effect of disorder is large. It is seen that at low temperatures the effect of disorder

is very large on both the Drude weight and the incoherent part of the kinetic energy. The Drude weight is rapidly suppressed while the incoherent part is enhanced a lot by the disorder site potential. At high temperatures where the Drude weight becomes very small, the disorder has little effect on the incoherent part of the kinetic energy. The effect of the disorder on the kinetic energy is even smaller because in this range of temperature the Drude weight slightly decreases while the incoherent part slightly increases with the introduction of the disorder.

We would address now the possible size effect on the results. In the Appendix-A we have derived a strong coupling effective polaronic hamiltonian where the different coefficients (in eq. A-2) have no size dependence provided the number of nearest neighbors ( $z$ ) is same. For a four-site system,  $z = 2$  which is same as that for an infinite 1-d chain. The kinetic energy in the ground state, obtained from Eq. (A2), for  $z = 2$  is given by

$$K_G = -2t_p - 4\frac{t_p^2}{\omega} \sum_{n,m=0;n+m \geq 1}^{\infty} \frac{g^{2(n+m)}}{n! m! (n+m)} - 4\frac{t_p^2}{\omega} \sum_{m=1}^{\infty} \frac{g^{2m}}{m! m} \quad (17)$$

where  $t_p = te^{-g^2}$ . The above clearly shows that for strong coupling the kinetic energy in the ground state should not have any size dependence if the number of nearest neighbors is same, hence the kinetic energy for  $N = 4$  will be same as that for an infinite lattice, where  $N$  is the number of lattice sites. This is completely consistent with the results obtained in a recent numerical study by Hohenberg et al.<sup>19</sup>. They obtained the same kinetic energy for  $N = 4, 8, 16, 32$  for large  $g$  while a small size effect is observed for small and intermediate coupling. With increasing temperature the size effect is even smaller as noted in Ref.19.

#### IV. Conclusions

We have investigated the effect of disorder and temperature on the properties of a polaron for a two- and four-site Holstein model. It has been observed that both the disorder and temperature reduce the polaron size and suppress the kinetic energy in the weak and intermediate  $e-ph$  coupling regime. For strong  $e-ph$  coupling polarons are practically immobile and the kinetic energy arises mainly from the to and fro motion of the (bare) electron between nearest-neighbor sites keeping the centre of the polaron fixed. In this regime the effects of disorder and temperature on the correlation functions and the kinetic energy are very small.

The polaronic kinetic energy has contributions from the coherent and the incoherent hopping processes. The contribution from the coherent hopping decreases with

increasing  $e-ph$  coupling, temperature and strength of the disorder. For small values of  $g$  and  $T$  this contribution (Drude weight) shows a weak suppression with  $g$  or  $T$  and then a rapid suppression with increasing  $g$  (or  $T$ ). The contribution from the incoherent hopping, on the other hand, increases with increasing  $g$  or  $T$  initially, reaches a maximum and then decreases. This contribution decreases as  $1/g^2$  with  $g$  in the strong coupling. In the regimes of strong coupling or high temperature the coherent contribution to the kinetic energy is very small compared to the incoherent contribution and the latter becomes almost independent of the disorder strength. We have also identified a cross-over temperature below which coherent part of the kinetic energy is dominant and above which the incoherent part is dominant. This cross over temperature decreases with the increase of the electron-phonon coupling.

The variation of the polaronic specific heat with respect to the  $e-ph$  coupling shows a peak in the intermediate  $e-ph$  coupling regime at low temperatures. A suppression of the specific heat due to disorder has been observed when  $e-ph$  coupling is in the weak or intermediate regime.

For the Holstein model the interaction is very short ranged and the size effect generally does not play a significant role in shaping different properties<sup>19,21,22</sup>. As pointed out previously the size effect on the kinetic energy is negligible for strong coupling, while the effect is finite but small for weak and intermediate coupling. At higher temperatures the size effect is even smaller. Regarding the role of the disorder on the Drude weight of the polaronic system, the size effect has not been reported to our knowledge. We find that for strong coupling or at higher temperatures the effect of disorder on the polaron dynamics is negligible, hence the size effect will also be negligible as similar to that for the ordered system. In other region of the coupling the qualitative behavior of the results presented here for the four-site system are expected to be the same for larger systems.

#### APPENDIX- A

Applying the standard Lang Firsov (LF) transformation to the Holstein model in Eq. (1) one obtains

$$\begin{aligned} \bar{H} &= e^R H e^{-R} \\ &= \sum_i (\epsilon_i - \epsilon_p) c_i^\dagger c_i - \sum_{i,j}' t_p c_i^\dagger c_j e^{g(b_i^\dagger - b_j^\dagger)} e^{-g(b_i - b_j)} \\ &\quad + \omega \sum_i b_i^\dagger b_i \end{aligned} \quad (A-1)$$

where  $R = \sum_i g n_i (b_i - b_i^\dagger)$ ,  $\epsilon_p = g^2 \omega$  is the polaron binding energy,  $t_p = e^{-g^2}$  is the polaronic hopping strength and  $j$  is a nearest neighbor of  $i$ .

The second term of Eq.(A-1) represents the kinetic energy operator which involves zero-phonon as well as

multiphonon processes (in the LF phonon basis) associated with the hopping of a polaron between nearest-neighbor sites. In the strong coupling limit, where  $t_p$  is very small, following a second order strong coupling perturbation theory an effective expression for the kinetic terms (within the phonon ground state) may be obtained as<sup>23</sup>

$$\begin{aligned}
H_{kin} &= -t_p \sum'_{i,j} c_i^\dagger c_j \\
&- 2zt_p^2 \sum_{n,m=0;n+m \geq 1}^{\infty} \frac{g^{2(n+m)}}{n! m! (n+m)\omega} \sum_i c_i^\dagger c_i \\
&- 2t_p^2 \sum_{n=1}^{\infty} \frac{g^{2m}}{m! m\omega} \sum_{i,k} c_i^\dagger c_k
\end{aligned} \tag{A-2}$$

where  $z$  is the number of nearest neighbors. The first term of  $H_{kin}$  represents the coherent hopping of polarons without emission or absorption of phonons, the second term originates from virtual hopping of a polaron from site  $i$  to a nearest neighbor site  $j$  and back. This hopping is associated with virtual emission of multi phonons at the sites  $i$  and  $j$  followed by absorption of all the emitted phonons while hopping back. In this process the (bare) electron within the polaron undergoes forward and backward motion between nearest-neighbor sites keeping the polaron immobile. Third term represents an effective hopping of a polaron from site  $i$  to a second nearest neighbor site  $k$  via a common nearest neighbor site  $j$  where multi phonons are created and then absorbed. For strong coupling the coefficients of the first and third terms in Eq. (A-2) become negligible and only the second term ( $\sim t^2/\epsilon_p$ ) contributes to the kinetic energy. In presence of disorder  $(n+m)\omega$  in the denominator of the second term modifies to  $(n+m)\omega \pm \epsilon_d$ , where  $\epsilon_d$  is the difference between the site potentials at sites  $i$  and  $j$ . The major contributions of this term for strong coupling comes from multi phonon processes with high values of  $(n+m)\omega$  such that  $(n+m)\omega \gg \epsilon_d$ . As a consequence of the above reasons the coefficient of the second term in (A2) as well as the kinetic energy in the strong coupling region becomes very weakly dependent on the disorder potential.

It may be mentioned that the Eq.(A2) is valid for any dimension and size of the system. The value of  $z$  would be different for different dimensions.

## APPENDIX- B

The Hamiltonian of the system in the broken time reversal symmetry may be written as

$$H(\phi) = - \sum_i (te^{i\phi} c_i^\dagger c_{i+1} + h.c) + V \tag{B-1}$$

where  $V$  is composed of electronic potential and interaction of electrons with lattice. Let  $H_0$  be the Hamiltonian of the system when  $\phi = 0$ , and the corresponding eigen energies and eigen states be  $E_n^0$  and  $|\psi_n^0\rangle$ , respectively. If  $E_n(\phi)$  be the eigen energy of the Hamiltonian  $H(\phi)$ , the Drude weight for the  $n$ -th eigen state of the Hamiltonian  $H_0$  is<sup>17</sup>

$$D_n = \frac{\partial^2 E_n(\phi)}{\partial \phi^2} \Big|_{\phi=0} \tag{B-2}$$

For small  $\phi$ ,  $H(\phi)$  can be expressed as

$$\begin{aligned}
H(\phi) &= H_0 - i\phi t \sum_i (c_i^\dagger c_{i+1} - c_{i+1}^\dagger c_i) \\
&+ \frac{\phi^2}{2} t \sum_i (c_i^\dagger c_{i+1} + c_{i+1}^\dagger c_i) + \dots
\end{aligned} \tag{B-3}$$

Considering the terms involving  $\phi$  as a perturbation a second order perturbation calculation gives

$$\begin{aligned}
E_n(\phi) &= E_n^0 - i\phi t \langle \psi_n^0 | (\sum_i c_i^\dagger c_{i+1} - c_{i+1}^\dagger c_i) | \psi_n^0 \rangle \\
&+ \phi^2 t^2 \sum_{n' \neq n} \frac{|\langle \psi_n^0 | (\sum_i c_i^\dagger c_{i+1} - c_{i+1}^\dagger c_i) | \psi_{n'}^0 \rangle|^2}{E_{n'}^0 - E_n^0} \\
&+ \frac{\phi^2 t}{2} \langle \psi_n^0 | \sum_i (c_i^\dagger c_{i+1} + c_{i+1}^\dagger c_i) | \psi_n^0 \rangle + \dots
\end{aligned} \tag{B-4}$$

Therefore

$$\begin{aligned}
D_n &= 2t^2 \sum_{n' \neq n} \frac{|\langle \psi_n^0 | (\sum_i c_i^\dagger c_{i+1} - c_{i+1}^\dagger c_i) | \psi_{n'}^0 \rangle|^2}{E_{n'}^0 - E_n^0} \\
&- K_n
\end{aligned} \tag{B-5}$$

where,

$$K_n = -t \langle \psi_n^0 | \sum_i (c_i^\dagger c_{i+1} + c_{i+1}^\dagger c_i) | \psi_n^0 \rangle \tag{B-6}$$

is the expectation value of the kinetic energy for the  $n$ -th eigen states of the Hamiltonian  $H_0$ . Taking the thermal average over all the eigenstates at a temperature  $T$  establish the sum rule

$$\begin{aligned}
-\frac{\langle K \rangle}{2} &= \frac{\langle D \rangle}{2} \\
&+ t^2 \left\langle \sum_{n' \neq n} \frac{|\langle \psi_n^0 | \sum_i (c_i^\dagger c_{i+1} - c_{i+1}^\dagger c_i) | \psi_{n'}^0 \rangle|^2}{E_n - E_{n'}} \right\rangle
\end{aligned} \tag{B-7}$$

where the thermal average of an observable  $A$  is

$$\langle A \rangle = \frac{\sum_n A_n \exp(-E_n/k_B T)}{\sum_n \exp(-E_n/k_B T)}. \tag{B-8}$$

In the above expression  $A_n$  is the expectation value of the observable  $A$  for the  $n$ -th eigen state of the Hamiltonian  $H_0$ .

- <sup>1</sup> J. P. Falck, A. Levy, M. A. Kastner, and R. J. Birgeneau, Phys. Rev. B **48**, 4043 (1993); XiangXin Bi and Peter C. Eklund, Phys. Rev. Lett. **70**, 2625 (1993).
- <sup>2</sup> G. Zhao, K. Conder, H. Keller and K. A. Muller, Nature **381**, 676 (1996); G. Zhao, M. B. Hunt, H. Keller and K. A. Muller, *ibid* **385**, 236 (1997).
- <sup>3</sup> R. G. Endres, D. L. Cox and R. R. P. Singh, Rev. Mod. Phys. **76**, 195 (2004).
- <sup>4</sup> A. N. Das and S. Sil, Physica C **207**, 51 (1993); J. Phys.: Condens. Matter **5**, 1 (1993).
- <sup>5</sup> A. N. Das and P. Choudhury, Phys. Rev. B **49**, 13219 (1994)
- <sup>6</sup> P. Choudhury and A. N. Das, Phys. Rev. B **53**, 3203 (1996).
- <sup>7</sup> E. Jeckelmann and S. R. White, Phys. Rev. B **57**, 6376 (1998).
- <sup>8</sup> G. Wellein and H. Fehske, Phys. Rev. B **58**, 6208 (1998).
- <sup>9</sup> M. Capone, S. Ciuchi and C. Grimaldi, Europhys. Lett. **42**, 523 (1998).
- <sup>10</sup> A. H. Romero, D. W. Brown, and K. Lindenberg, Phys. Rev. B **59**, 13728 (1999).
- <sup>11</sup> J. Bonca, S. A. Trugman and I. Batistic, Phys. Rev. B **60**, 1633 (1999).
- <sup>12</sup> J. Chatterjee and A. N. Das, Phys. Rev. B **61**, 4592 (2000).
- <sup>13</sup> O. S. Barisic, Phys. Rev. B **65**, 144301 (2002).
- <sup>14</sup> M. Zoli and A. N. Das, J. Phys.: Condens. Matter **16**, 3597 (2004).
- <sup>15</sup> J. Chatterjee and A. N. Das, Eur. Phys. J. B **46**, 481 (2005).
- <sup>16</sup> A. N. Das and S. Sil, Phys. Letts. A **348**, 266 (2006).
- <sup>17</sup> W. Kohn, Phys. Rev. **133**, A171 (1964).
- <sup>18</sup> J. Ranninger and U. Thibblin, Phys. Rev. B **45**, 7730 (1992)
- <sup>19</sup> M. Hohenadler, H. G. Evertz, and W. von der Linden, Phys. Rev. B **69**, 024301 (2004).
- <sup>20</sup> H. Fehske, J. Loos and G. Wellein, Phys. Rev. B **61**, 8016 (2000).
- <sup>21</sup> M. Capone and S. Ciuchi, Phys. Rev. B **65**, 104409 (2002).
- <sup>22</sup> Y. Takada and A. Chatterjee, Phys. Rev. B **67**, 081102 (2003).
- <sup>23</sup> A. H. Romero, D. W. Brown, and K. Lindenberg, Phys. Rev. B **60**, 4618 (1999).

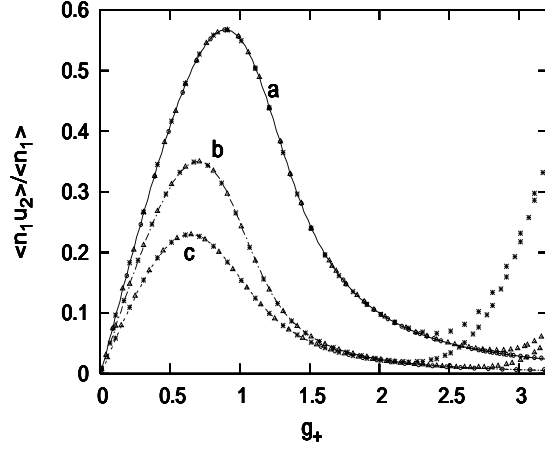


FIG. 1. Convergence of the correlation function  $\langle n_1 u_2 \rangle / \langle n_1 \rangle$  ( $u_2 = b_2 + b_2^\dagger$ ) for the two-site system. (a) Solid line:  $t = 2.1$ ,  $\epsilon_d = \epsilon_2 - \epsilon_1 = 1.0$  with  $n_p = 40$ ; (b) dashed line :  $t = 1.0$ ,  $\epsilon_d = 0.5$  with  $n_p = 40$ ; (c) dash-dotted line :  $t = 1.0$ ,  $\epsilon_d = 1.0$  with  $n_p = 40$ . Solid squares are for  $n_p = 15$ , solid triangles are for  $n_p = 20$ , solid circles are for  $n_p = 25$ . All energy parameters are expressed in units of  $\omega = 1$ .

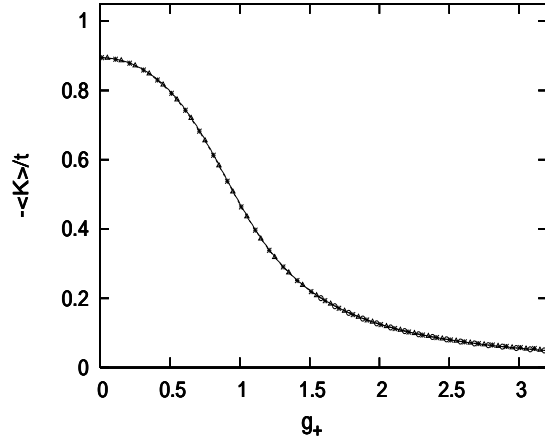


FIG. 2. Convergence of the kinetic energy  $-\langle K \rangle / t$  for the two-site system. Solid line:  $t = 1.0$ ,  $\epsilon_d = 1.0$  with  $n_p = 40$ , solid squares are for  $n_p = 15$ , solid triangles are for  $n_p = 20$ , solid circles are for  $n_p = 25$ . All energy parameters are expressed in units of  $\omega = 1$ .

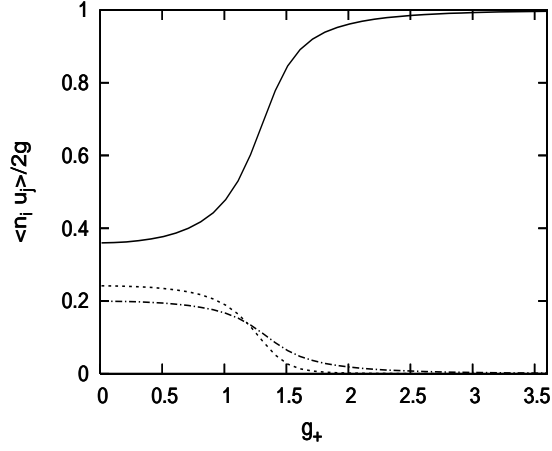


FIG. 3. Variation of  $\langle n_i u_j \rangle / 2g$  with  $g_+$  for  $t = 2.1$  and  $\epsilon_d = 1.0$  for the two-site Holstein model. Solid line:  $\langle n_1 u_1 \rangle / 2g$ , dashed line:  $\langle n_2 u_2 \rangle / 2g$  and dash-dotted line:  $\langle n_1 u_2 \rangle / 2g = \langle n_2 u_1 \rangle / 2g$ .

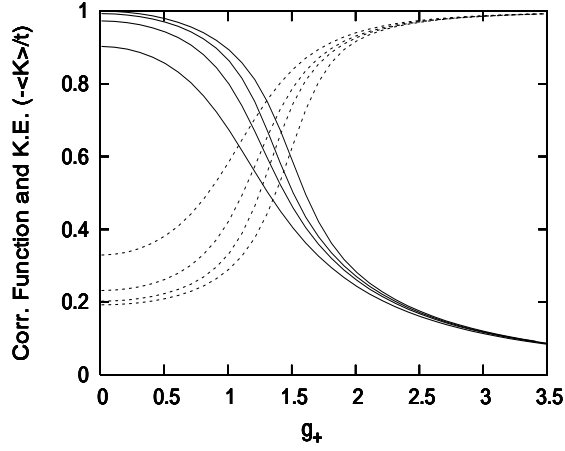


FIG. 4. Variation of the kinetic energy  $-\langle K \rangle / t$  (solid lines) and the correlation function  $\chi_d^{avg}$  (dashed lines) with  $g_+$  for  $t = 2.1$  and different  $\epsilon_d$  for the two-site Holstein model. Solid lines from top to bottom and dashed lines from bottom to top are for  $\epsilon_d = 0, 0.5, 1.0$  and  $2.0$ , respectively.

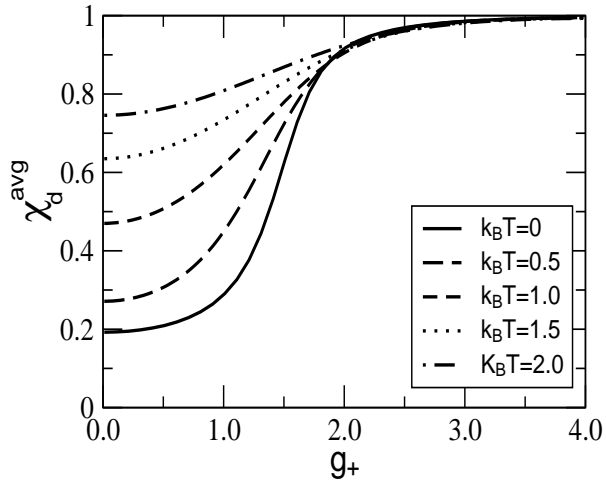


FIG. 5. Variation of  $\chi_d$  with  $g_+$  for the ordered case ( $\epsilon_d = 0$ ) for different temperatures. Solid line:  $k_B T = 0$ , long dashed line:  $k_B T = 0.5$ , short dashed line:  $k_B T = 1.0$ , dotted line:  $k_B T = 1.5$ , dash-dotted line  $k_B T = 2.0$ .  $t = 2.1$  in the energy scale of  $\omega=1$ .

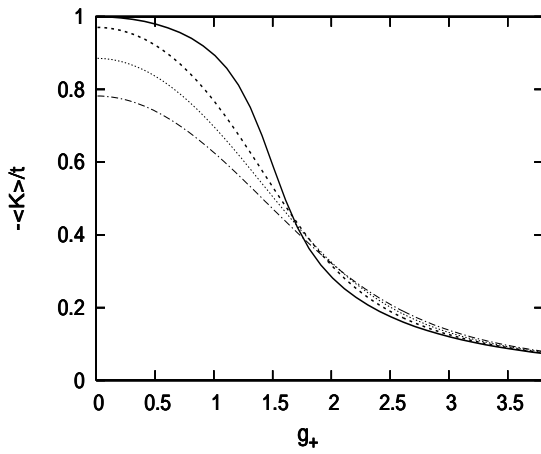


FIG. 6. Variation of the kinetic energy  $-\langle K \rangle / t$  with  $g_+$  for the ordered case for different temperatures. Solid line:  $k_B T = 0$ , short dashed line:  $k_B T = 1.0$ , dotted line:  $k_B T = 1.5$ , dash-dotted line  $k_B T = 2.0$ .  $t = 2.1$  in the energy scale of  $\omega=1$ .

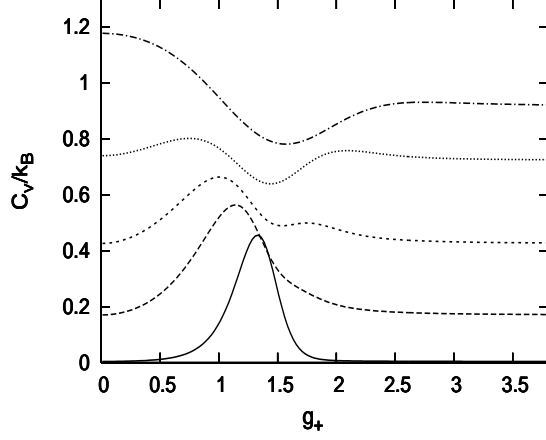


FIG. 7. Variation of the specific heat ( $C_v/k_B$ ) with  $g_+$  for the ordered two-site Holstein model for different temperatures. Solid line:  $k_B T = 0.1$ , long dashed line:  $k_B T = 0.2$ , short dashed line:  $k_B T = 0.3$ , dotted line:  $k_B T = 0.4$ , dash-dotted line:  $k_B T = 0.5$ .  $t = 2.1$  in the energy scale of  $\omega = 1$ .

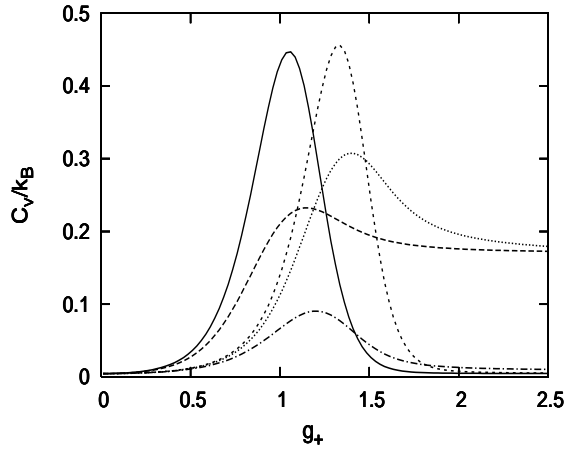


FIG. 8. Variation of the specific heat ( $C_v/k_B$ ) with  $g_+$  at a temperature  $k_B T = 0.1$  for ordered and disordered two-site Holstein model for different hopping parameters. Solid line:  $t = 1.0, \epsilon_d = 0$ ; long dashed line:  $t = 1.0, \epsilon_d = 0.5$ ; short dashed line:  $t = 2.1, \epsilon_d = 0$ ; dotted line:  $t = 2.1, \epsilon_d = 0.5$ ; dash-dotted line:  $t = 2.1, \epsilon_d = 1.0$ .

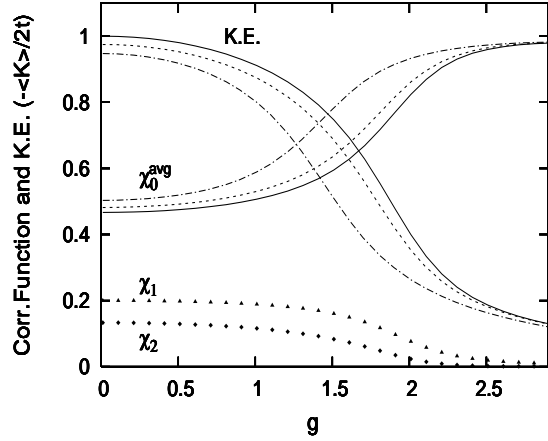


FIG. 9. Variation of the kinetic energy  $-\langle K \rangle / 2t$  and the correlation function  $\chi_0^{avg}$  with  $g$  in the ground state for ordered and disordered four-site Holstein model. Solid lines: ordered case, dashed lines: disordered with site potentials  $(1,0,0,0)$ , dash-dotted curves: site potentials  $(-1,0,0,0)$ . Solid triangles and diamonds represent  $\chi_1$  and  $\chi_2$ , respectively for the ordered case. Value of the hopping parameter used  $t = 1.0$  in the energy scale of  $\omega = 1$ .

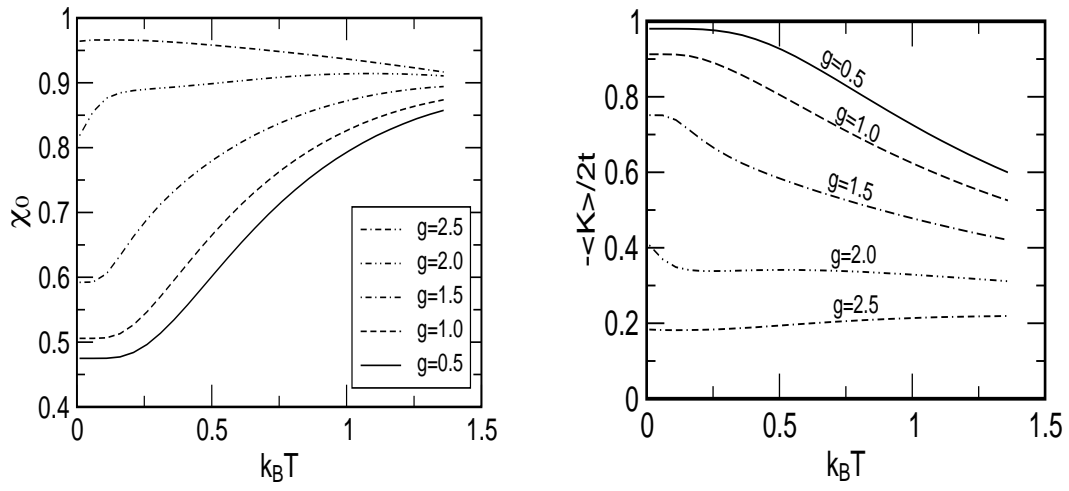


FIG. 10. Variation of  $\chi_0$  and the kinetic energy  $-\langle K \rangle / 2t$  with temperature for the ordered four-site Holstein model for different values of  $g$ . Value of the hopping parameter used  $t = 1.0$  in the energy scale of  $\omega=1$ .

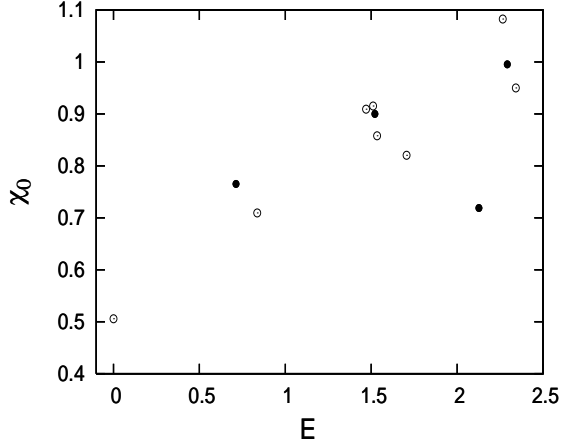


FIG. 11. Values of the on-site correlation function ( $\chi_0$ ) for the ground and the excited states for  $g = 1$  and  $t = 1$  for the ordered four-site Holstein model shown up to  $E = 2.4$ , where  $E$  is the energy of the excited state measured from the ground state energy. There are sixteen states within the energy range  $0 \leq E \leq 2.4$ . Four states have double degeneracy (shown by solid circles).

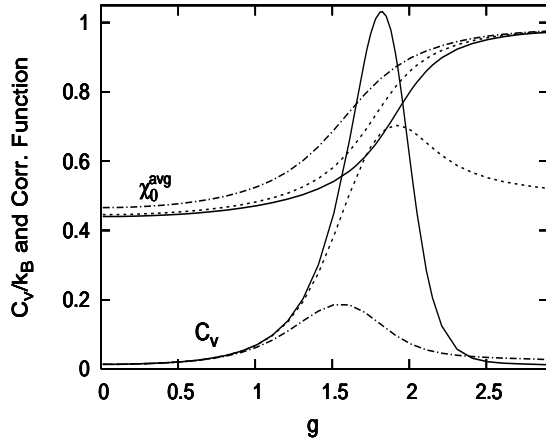


FIG. 12. Variation of the specific heat ( $C_v/k_B$ ) and the correlation functions  $\chi_0^{avg}$  with  $g$  at a temperature  $k_B T = 0.1$  for  $t = 1.2$  for different set of site potentials for four-site Holstein model. Solid lines: ordered case, dashed line: disorderd case with site potentials  $(-0.5, 0, 0, 0)$  and dash-dotted line: disorderd case with site potentials  $(-1, 0, 0, 0)$ .

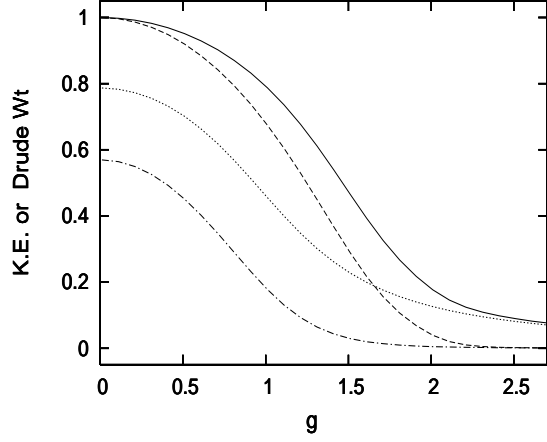


FIG. 13. Variation of the kinetic energy  $-\langle K \rangle / 2t$  and the Drude weight with  $g$  in the ground state for ordered and disordered cases for  $t=0.5$ . Ordered case: Kinetic energy (solid line), Drude weight (dashed line). Disordered case with site potentials  $(-1,0,0,0)$ : Kinetic energy (dotted line), Drude weight (dash-dotted line).

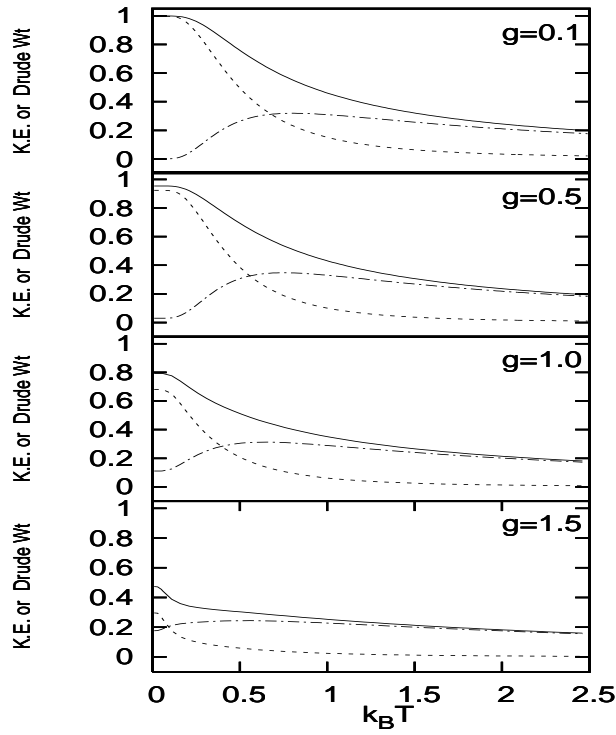


FIG. 14. Variation of the kinetic energy  $-\langle K \rangle / 2t$  (solid lines) and the Drude weight  $(D/2t)$  (dashed lines) with  $k_B T$  for the ordered lattice for different values of  $g$ . The dot-dashed lines represent the incoherent part of the kinetic energy. Value of the hopping parameter used  $t=0.5$ .

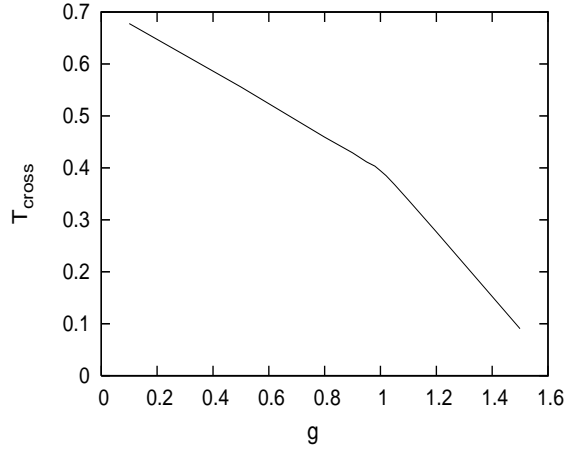


FIG. 15. Variation of the cross-over temperature ( $T_{cross}$ ) with  $g$  for  $t=0.5$  for the ordered case.

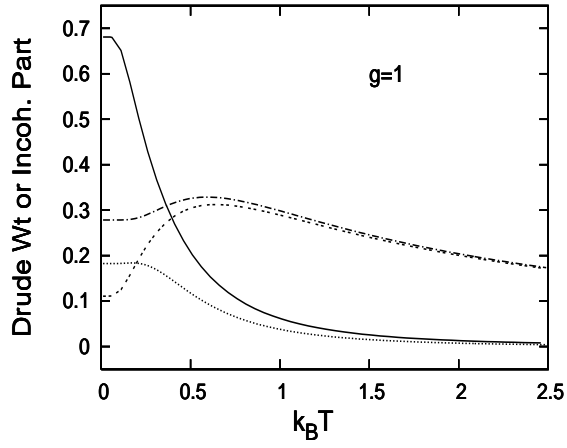


FIG. 16. Variation of the Drude weight and the incoherent part of the kinetic energy (in a scale of  $2t$ ) with temperature for ordered and disordered cases for  $t=0.5$ . Ordered case: Drude weight (solid line), incoherent part of the K.E. (dashed line). Disordered case with site potentials  $(-1,0,0,0)$ : Drude weight (dotted line), incoherent part of the K.E. (dash-dotted line).